"Direct Dynamics Method for the Calculation of Reaction Rates," D. G. Truhlar, in *The Reaction Path in Chemistry: Current Approaches and Perspectives*, edited by D. Heidrich (Kluwer, Dordrecht, 1995), pp. 229-255. [Understanding Chem. React. **16**, 229-255 (1995).]

DIRECT DYNAMICS METHOD FOR THE CALCULATION OF REACTION RATES

DONALD G. TRUHLAR
Department of Chemistry and Supercomputer Institute
University of Minnesota
Minneapolis, Minnesota 55455-0431

1. Introduction

Accurate quantum dynamics calculations for atom-diatom reactions have advanced to the stage where the nuclear-motion Schrödinger equation can be solved essentially exactly for a given potential energy surface [1]. For example, we recently reported accurate quantum mechanical rate constants for the reaction $D + H_2 \rightarrow HD + H$ over a wide temperature range [2]. In this case the potential energy surface is very well known, and the dynamical results for the most accurate potential energy surface [3] agree with experiment [4] within 12% (maximum deviation) over the 200–900K temperature interval, with slightly large errors at higher T (16% at 1300 K, 22% at 1500 K). This is quite satisfying for a totally *ab initio* calculation of a chemical reaction rate.

Unfortunately, accurate quantum dynamics calculations are beyond the state of the art for systems with 5 or more atoms. But the atom-diatom calculations can be used to test the accuracy of more practical theories. For example, a 1986 calculation [5] based on variational transition state theory (VTST) with semiclassical tunneling (ST) contributions agrees with the accurate quantum dynamical results[2] within 10–20% over the whole 300–1500 K range of T. This is particularly encouraging for two reasons: (i) VTST/ST calculations provide an easily understood and classically visualizable picture of dynamical bottlenecks and tunneling paths [6]; (ii) VTST/ST calculations are practical for much larger systems [7].

VTST [8] provides a generalization of conventional transition state theory [6a,9] (TST). A conventional TST calculation is equivalent to calculating the one-way flux through a phase space hypersurface that divides reactants from products and passes, perpendicular to the imaginary-frequency normal mode, through the highest-energy saddle point of the potential energy on the lowest-energy path from reactants to products [6c]. In VTST one still calculates a one-way flux through a hypersurface that separates reactants from products, but now the location and orientation of the dividing surface are chosen, in

D. Heidrich (ed.), The Reaction Path in Chemistry: Current Approaches and Perspectives, 229–255.

accordance with the fact that this flux provides a classical upper bound to the equilibrium reaction rate, to minimize the one-way flux [6c,10]. Where the variation is carried out for a thermal rate constant, i.e., when the flux is calculated for a canonical ensemble, this is called canonical variational transition-state theory (CVT). A practical way to accomplish this variation of the dividing surface is to consider a one-parameter sequence of dividing surfaces locally orthogonal to a reaction path, with the parameter being the distance s along the path at which the surface intersects the path [8j,8k,10,11].

To carry out a VTST calculation, one first defines a reaction coordinate s. In our work we define this as the union of the paths of steepest descents from the saddle point (which is the conventional transition state) towards reactants and towards products, where these paths are computed in an isoinertial coordinate system [12], e.g., normal coordinates of the saddle point [12a,12d,12e]. (An isoinertial coordinate system is any system in the kinetic energy has the form $\sum_{i=1}^{F} p_i^2/2\mu$, where μ is a common reduced mass for all degrees of freedom.) The union of these paths is called [12d,12e] the minimum-energy path (MEP); some workers call it the intrinsic reaction path, or less suitably, the intrinsic reaction coordinate [12f].

The calculation of the one-way classical flux through the dividing surface at s reduces to

$$\text{Flux} = k[\text{X}][\text{Y}] \tag{1}$$

where k is the rate constant, [X] and [Y] are concentrations of the bimolecular reactants (for a unimolecular reaction one gets the same results without [Y]), and [6c,8k]

$$k = \frac{k_B T}{h} K_C^{GT}(s) \tag{2}$$

where k_B is Boltzmann's constant, T is temperature, h is Planck's constant, and $K_C^{GT}(s)$ is the classical equilibrium constant for

$$\text{X} + \text{Y} \longleftrightarrow \text{GTS}(s) \tag{3}$$

where GTS(s) is a species in which one degree of freedom is suppressed by constraining the value of the reaction coordinate to be s. Although GTS(s) is not an ordinary species, it is conventional, dating back to Eyring's 1935 paper [13], to replace $K_C^{GT}(s)$ by a quantal equilibrium constant, in which the levels of X, Y, and GTS(s) are quantized. This was justified as the leading term in a semiclassical series by Wigner [14], but it is neither rigorous nor unique. Recently though it has been shown [15] that short-lived resonances occur at maxima in vibrationally adiabatic potentials, with a spectrum

corresponding very closely to the quantized energy levels usually assumed for GTS(*s*). These states are broadened in accordance with their finite lifetimes, and the broadening may also be interpreted as a consequence of tunneling [15]. The level widths for H + H_2 [15a] are several k_BT below the transition state theory thresholds, which leads to large rate enhancements.

For the D + H_2 reaction, the VTST/ST calculations mentioned above [5] indicate that tunneling increases the rate constant by factors of 3, 7, and 60 at 400, 300, and 200 K, respectively. This confirms that tunneling is an important ingredient in accurate reaction rate calculations. Table 1 shows similar rate enhancements for several other gas-phase hydrogen-atom transfer reactions we have studied in recent years, namely, the H + H_2 reaction [16], the 1,5 sigmatropic shift in *cis*-pentadiene [7b], the CF_3 + CH_4 reaction, [17] and the OH + CH_4 reaction [18]. I anticipate similarly large below-threshold tunneling contributions for many H, H^+, and H^- transfer reactions in both the gas phase and solution.

We have found that several ingredients are required for an accurate semiclassical calculation of tunneling contributions to chemical reaction rates [7b,10a,16,17,19], and we have developed multidimensional semiclassical tunneling methods to calculate such

Table 1. Rate constant including tunneling divided by rate constant without tunneling for four reactions at various temperatures.

T(K)	k(VTST/ST) + k(VTST)
H + H_2	
250	60
300	20
500	3
1,5 sigmatropic shift in *cis*-pentadiene	
500	6
CF_3 + CH_4	
300	200
400	20
500	7
OH + CH_4	
250	20
300	7
400	$2\frac{1}{2}$

tunneling contributions [7b,10a,16,17]. A critical element in making such calculations practical is that for motion in the vicinity in the minimum-energy path we base the tunneling calculation

on the ground-state vibrationally adiabatic [12b,12d,12e,20] potential energy curve, called $V_a^G(s)$. The calculation of $V_a^G(s)$ assumes that vibrational motions transverse the reaction path adjust adiabatically to reaction-path motion and hence retain their quantum number (not their energy) [12b,12d,12e]. This is justified by the reaction-coordinate motion being in a threshold region. Analysis of accurate quantal calculations confirms, furthermore, that at the lowest energies at which reaction occurs, the flux emanating from several low-energy reactant states all tends to pass through the transition state [15b,21] region in the ground vibrational state. The kinetic energy operator to associate with $V_a^G(s)$ is not, however just $-(\hbar^2 / 2\mu)d^2 / ds^2$. Because the MEP is curved, there is an internal centrifugal effect. Unlike the classical centrifugal force, which points to the convex side of a curved path (bobsled effect [12b]), in quantal tunneling regions the centrifugal force is toward the concave side of the path, and it causes corner cutting [12b,19a,22].

For small curvature of the reaction path, we have found, generalizing Marcus and Coltrin's treatment [23] of collinear H + H_2, that these negative internal centrifugal effects may be treated accurately [19c,19e,19f] even for multidimensional systems in terms of a single dominant tunneling path [19a]. We developed a quantitative multidimensional treatment based on an implicit effective path that cuts the corner to no greater extent in any transverse mode than the distance from the MEP to that mode's concave-side ground-state turning point [24]. Thus we calculate an action integral along an implicit path at or inside of the concave-side vibrational turning point in the direction of the internal centrifugal force (this force picks out, for each s, a particular linear combination of vibrational mode direction along which corner cutting occurs) [7b,24]. The path is implicit because the quantity directly approximated is the effective reduced mass, not the tunneling path. The method is called the small-curvature tunneling (SCT) approximation for short or centrifugal dominant small-curvature semiclassical adiabatic (CD-SCSA or CD-SCSAG) approximation for completeness (the G in the latter acronym stands for ground-state, and is included when the CD-SCSA algorithm is used to calculate ground-state transmission coefficients).

When reaction-path curvature is large, the situation is more complicated [19b,19d,24,25]. In this case, there may be significant contributions for a range of tunneling paths, the tunneling in the exoergic direction of reaction may proceed directly into vibrationally excited states of the products, and the tunneling paths may proceed through regions farther from the MEP than the transverse vibrational turning point, the radius of curvature of the reaction path, or both. In the general case, points along the dominant tunneling paths cannot be described in terms of an expansion of the potential about the MEP. The wider region covered by significant tunneling paths in the large-curvature case is called the

reaction swath. In our calculations we switch smoothly from reaction-path coordinates to local $3N$-dimensional Cartesians in this region. For large-curvature cases we calculate action integrals in the exoergic direction, including tunneling into quasidiabatic states of the product, along series of straight-line paths satisfying a resonance condition[19d,24,26]. The semiclassical algorithm for tunneling calculations in large-curvature cases is called the large-curvature tunneling (LCT) approximation for short or the large-curvature version-3 (LC3 or LCG3) approximation to be more precise (the G in the latter acronym stands for ground-state, and is included when the LC3 algorithm is used to calculate ground-state transmission coefficients).

Often it is not possible to tell a priori whether the SCT or LCT approximation is most appropriate. Typically a poor choice of tunneling path will underestimate the tunneling, a result which can be understood by identifying the optimum semiclassical tunneling path with the path of least imaginary action [26]. Thus we employ an approximation called the microcanonical optimized multidimensional tunneling approximation (μOMT) [17]. In this method, for each total energy we calculate the tunneling probability by both the SCT and LCT approximations, and we accept whichever gives the larger tunneling probability as the better result.

Whenever one includes tunneling one should also include nonclassical reflection [27]. Just as tunneling represents the quantum mechanical phenomenon by which a system with less energy than the maximum of the effective potential is nevertheless transmitted past it, nonclassical reflection is the quantum mechanical (diffraction) effect by which a system with more energy than the maximum of the effective potential is nevertheless reflected. Because these effects partially cancel, one should not include one without the other. Because the Boltzmann factor is bigger in the tunneling region, the result is that tunneling usually dominates nonclassical reflection, and it is common to mention only tunneling when speaking of the net effect. The net factor by which these two effects increase (or decrease) the reaction rate is called the transmission coefficient.

2. Dynamical methods

The dynamics methods we employ are reviewed above, and full details are presented elsewhere. In particular, the polyatomic variational transition state theory calculations are described briefly in the original journal article [28] and in full detail in a book chapter [10]. The SCT, LCT, and μOMT tunneling methods are also explained elsewhere [7b,17,24,25]. VTST and these multidimensional tunneling methods are also summarized in the chapter by Isaacson in the present volume.

The discussion so far has concentrated on the calculation of bimolecular rate constants for gas-phase reactions under thermal conditions. Many extensions, e.g., unimolecular reactions [10], microcanonical ensembles [8j,8l,10,29], and state-selected reactions [19c,30] are described elsewhere but are not reviewed here.

At this point we review the information needed for the dynamics calculations described above. The essential input to the dynamics calculations can all be calculated from the masses of the atoms and a potential energy surface (also called a potential energy function or the Born-Oppenheimer potential.)*

First we must find (in the language of electronic structure codes—optimize) the saddle point and calculate its energy (which is called $V^{\neq}$ when measured with respect to the motionless state of reactants) and hessian. From the geometry we calculate moments of inertia, and from the hessian we calculate vibrational frequencies. Similarly we calculate the geometry, energy, moments of inertia, and vibrational frequencies for reactants.

Then we calculate the MEP in the direction toward the reactant or reactants (negative s) and in the direction toward product or products (positive s). This may be done by following the negative gradient [8k,8l,10,20e] (Euler method), following the negative gradient with added stabilization steps [12d,32], or by various [32c,32d,32e,33] more sophisticated (though not necessarily more efficient) algorithms. Typically this requires a small step size, called the gradient step size δs. At a series of points along the MEP, spaced by the generalized normal mode stepsize Δs ($\geq \delta s$), we calculate the Hessian and carry out a generalized normal mode analysis to find the transverse vibrational directions and frequencies. These transverse vibrational modes are localized to the $(3N-7)$-dimensional space ($3N-6$ for a linear molecule) that is orthogonal to the MEP [11], as well as to overall translation and rotation, which is accomplished conveniently by restricting attention to the coordinate hyperplane perpendicular to the tangent to the reaction path [8j] or by diagonalizing a projected force constant matrix in isoinertial coordinates [34].

We estimate the electronic partition functions of reactants and products from the degeneracies and excitation energies of low-lying electronic states. Typically only the ground electronic state needs to be included for closed-shell species and only fine structure excited states (e.g., $^2P_{1/2}$ for halogens, $^2\Pi_{1/2}$ for OH) need be included for open-shell species.

In general reactant properties are denoted by a superscript R, for the supersystem of X and Y, or by separate superscripts X and Y, conventional transition state properties are denoted $\neq$, and generalized transition state properties are denoted by the superscript GT and/or by affixing the arguments s.

From the energies, moments of inertia, symmetry numbers, vibrational frequencies ω_i^R and $\omega_i(s)$, and reduced moments of inertia (the latter if one or more vibrations is

---

*The gradient field of the potential energy surface is the force field.

treated as a hindered internal rotor), we calculate the vibrationally adiabatic ground-state potential curve as [8l,10,20d,28]

$$V_a^G(s) = V_{MEP}(s) + \frac{1}{2}\hbar\left[\sum_m^{F^{GT}-1} \omega_m(s) - \sum_{m=1}^{F^X} \omega_m^X - \sum_{m=1}^{F^Y} \omega_m^Y\right] \quad (4)$$

where F is the number of internal degrees of freedom ($3N$–6 for a general species and $3N$–5 for a liner species) The generalized standard-state free energy of activation profile is computed as [20e,35]

$$\Delta G^{GT,0}(s) = V_{MEP}(s) + G^{GT,0}(T,s) - G^{R,0}(T) \quad (5)$$

$V_{MEP}(s)$ is the Born-Oppenheimer potential energy along the MEP. The standard-state free energy of reactants $G^{R,0}(T)$ is computed by well known formulas, and $G^{GT,0}(T,s)$ is computed similarly, but excluding contributions from the reaction coordinate s.

In calculating $G^{GT,0}(T,s)$ and $G^{R,0}$, vibrations that correspond to hindered internal rotations are singled out for special attention, and a correction for their anharmonicity is added using a one-dimensional model [17,24,36]. Multiple saddle points due to hindered internal rotation or symmetry are handled in calculating $G^{GT,0}(T,s)$ by standard use of symmetry numbers.

The canonical variational transition-state theory (CVT) rate constant is given by

$$k^{CVT}(T) = \frac{k_B T}{h} K^{\neq,0} \exp\left[-\max_s \Delta G^{GT,0}(T,s) \Big/ k_B T\right] \quad (6)$$

where for bimolecular reactions $K^{\neq,0}$ is the reciprocal of the concentration in the standard state. (For unimolecular reactions it is unity).)

The final predicted rate constant, including tunneling, is given by

$$k^{CVT/T}(T) = \kappa(T) k^{CVT}(T) \quad (7)$$

In the small-curvature tunneling approximation, $\kappa(T)$ requires, in addition to some of the information detailed above, the curvature components $C_m(s)$ of the curvature of the reaction path, where each curvature component measures the projection of the curvature vector on a particular generalized normal mode direction m. Calculation of $\kappa^{LCT}(T)$ or $\kappa^{\mu OMT}(T)$ requires, in addition, values of the Born-Oppenheimer potential V in the reaction swath, typically at points where it cannot be computed from the available harmonic expansion around the MEP.

3. Interfacing the dynamics calculations to the potential energy surface

We have employed four general strategies for obtaining potential energy surface information for reaction-path dynamics calculations, and these are discussed in this section in chronological order of their development.

3.1. ANALYTIC POTENTIAL ENERGY SURFACES

The most obvious way to specify a potential energy surface is as an analytic function of the coordinates. Typically such a function is obtained by semiempirical valence bond theory and/or a valence force field with bond breaking terms or by a fit to *ab initio* electronic structure calculations of the Born-Oppenheimer potential energy surface as a function of internuclear distances. This kind of analytic potential has been widely employed for systems with three atoms and less widely so for systems with 4–12 atoms [37]. Some recent examples include surfaces for the reactions H + CH_4 [38], $Cl^-(H_2O)_2$ + CHCl [7a,39], F + H_2 [40], and H + HBr [41].

The difficulty with this approach is that it is very time consuming and typically unsystematic. For polyatomics, the functional forms may suffer from missing or inadequate stretch-stretch or stretch-bend couplings. Even for triatomics, the barrier shape may depend strongly on the chosen functional form. One requires many electronic structure calculations and considerable care to create an accurate (or even useful) surface with all the important internal-coordinate couplings and without artifacts or spurious features.

The methods presented next attempt to circumvent the laborious and painstaking fitting process in one way or another. These methods may all be called direct dynamics in that the dynamics calculations are based *directly* on the electronic structure data without the intermediary of a fit. The first of the methods (section 3.2) is called straight direct dynamics because it is an implementation of this approach in its purest and most straightforward form.

3.2. STRAIGHT DIRECT DYNAMICS

In a second approach, called direct dynamics, we carry out the dynamics calculation precisely the same way as when using an analytic potential energy function, but whenever a potential energy, gradient, or hessian is needed, it is calculated by a full electronic structure calculation, employing *ab initio* methods [42], *ab initio* plus scaled-correlation methods [43], density functional or tight-binding theories [44], or semiempirical neglect-of-differential overlap methods [45]. The direct dynamics approach was originally employed for classical mechanical dynamics calculations [46] in which context it has received considerable further development [47]. Direct dynamics methods have also been employed for trajectory surface hopping calculations [48]. The present chapter is concerned with semiclassical direct dynamics based on reaction paths or reaction swaths;

several examples of this kind of calculations have been reported, both in our group [7b,17,32d,49] and by others [50], and reviews [51] of some of this work are available as well.

One difficulty with straight direct dynamics is that the large number of electronic structure calculations required tends to mitigate against employing high levels of theory. Thus, for example, some direct dynamics calculations have employed minimum basis sets [32d] and semiempirical molecular orbital theory [7b].

One way to keep the cost of the calculations low but improve the accuracy is to use semiempirical molecular orbital calculations in which some of the parameters are fit to data for the specific reaction of interest or for a limited range of reactions. We call this approach SRP for specific reaction parameters or specific range parameters. In several applications we have combined the SRP approach with semiempirical molecular orbital theory employing the neglect of diatomic differential overlap (NDDO) approximation. This is called the NDDO-SRP approach [49].

The NDDO parameters may be adjusted using experimental exoergicities, activation energies, rate constants, and/or reagent geometries and frequencies or by using higher-level *ab initio* data at selected stationary points or other geometries. Alternatively one can use some combination of experimental and *ab initio* data, with the combination depending on availability of data and feasibility of high-level calculations. The parameters may be adjusted by trial and error [17,49a,49b,49c,49d] or by an optimization routine, for example by a genetic algorithm [49e].

The reaction $CF_3 + HCD_3 \rightarrow CF_3H + CD_3$ provides a prototype example of the use of the NDDO-SRP approach [17].

One difficulty with this approach is that, although it is not very difficult to adjust a few NDDO parameters to improve the predicted barrier height and exoergicity, one must be careful not to introduce spurious wells or spuriously deep wells in the potential energy surface or to make the predicted reactant and product geometries or vibrational frequencies unphysical. Furthermore, if one tries to adjust the NDDO parameters to also improve the saddle point and/or reagent frequencies, the task becomes considerably more difficult. As one practical solution to this problem, we have found [49e,52] that genetic algorithms [53] are a useful technique for this difficult parameter adjustment. (Genetic algorithms are the most well known members of the larger set of evolutionary strategies [54] for nonlinear optimization.)

3.3. INTERPOLATED VARIATIONAL TRANSITION STATE THEORY (IVTST)

We have developed another approach to direct dynamics that we call interpolated variational transition state theory (IVTST) [55]. In this approach we carry out electronic structure calculations, including energies, gradients, and hessians, at the reactants,

products, saddle point, and zero, one, or two additional points near the saddle point. These additional points are obtained by taking a step along the MEP in the direction of reactants or products or both. All other information needed for VTST calculations with SCT transmission coefficients is obtained by interpolation from this data.

The IVTST method was tested [55] for the OH + H_2 and CH_3 + H_2 reactions and six isotopomeric analogs by using previously available [38,56] analytic potential energy functions for these systems. To carry out the tests we pretended that we know the potential energy surface data only at the three stationary points (reactions, products, and saddle point) and zero, one, or two additional points on the MEP near the saddle point. The rest of the surface information was interpolated. The tests were very encouraging at the level of variational transition state theory without tunneling or including zero-curvature tunneling. Small-curvature tunneling calculations were also carried out and were less accurate in some cases due primarily to the difficulty of interpolating the effective reduced mass quantitatively in regions where its shape is qualitatively correct.

The IVTST method is presently developed only for small-curvature tunneling. Since large-curvature tunneling often proceeds through regions far from the MEP, it is not clear if this could be interpolated reliably using only the data used for the presently developed interpolation schemes. Further work to extend the IVTST method to large-curvature systems would be desirable.

Even for small-curvature tunneling, a difficulty with the IVTST method as applied so far is that the nonstationary points on the MEP are very near the saddle point. This is primarily a matter of economics since it is less expensive to follow the MEP only a short distance. This could be circumvented in the future by various strategies. For example, one could take a few or several gradient-only points with $\delta s < \Delta s$ before calculating the additional nonstationary-point hessians, or one could generalize the method to use points off the MEP.

The IVTST method has been applied successfully to the reactions Cl + CH_4 [55], OH + CH_4 [18], OH + CD_4 [57], and OH + C_2H_6 [7d]. Because these applications were very successful, and because IVTST can be incorporated into electronic structure codes in a very systematic and general way, IVTST may often be the method of choice for future applications. Hence further development of the method would probably be very useful. Nevertheless we are currently even more enthusiastic about dual-level schemes, which are discussed next.

3.4. DUAL-LEVEL DYNAMICS

Our third generation direct dynamics scheme is called VTST with interpolated corrections (VTST-IC) or dual-level direct dynamics (DLDD) or triple-slash (///) dynamics. This approach involves three steps [49c]:

(1) First, using straight direct dynamics with a low level (LL) of electronic structure theory, we perform full VTST calculations with optimized multidimensional tunneling, including frequencies along the reaction path and large-curvature tunneling through the reaction swath.

(2) Then, using a high level (HL) of electronic structure theory, we carry out energy and frequency calculations at 3 or 4 stationary points.

(3) In the final step we use the HL calculations to interpolate corrections to the energies, frequencies, and moments of inertia of the LL ones.

If HL denotes the high level (e.g., QCISD(T)/aug-cc-pVTZ or QCIS(T)/aug-cc-pVTZ//MP2/aug-cc-pVTZ) and LL denotes the low level (e.g., NDDO-SRP or MP2/6-31G*), then the final result of these three steps is denoted HL///LL, which is a direct generalization of the // notation of electronic structure theory. In particular //LL means that stationary point geometries are calculated at level LL, whereas ///LL mans that the reaction path is calculated at level LL.

In step (1) we calculate geometries, reaction-path curvature, and energies along the MEP, we obtain the generalized normal modes orthogonal to the MEP, including s-dependent frequencies and mode directions, and for large-curvature tunneling we calculate energies in the corner-cutting swath. In our VTST-IC algorithm [49c] we correct all the energies and frequencies but only two aspects of the geometries, namely the moments of inertia for the rotational partition functions and the reduced moments of inertia for the hindered internal rotation(s), if present. The geometries, however, are an intrinsic source of the reaction-path curvature and the mode directions (which affect the tunneling calculations) and these are not corrected. Thus it is very important that the low-level calculation give reasonable geometries along the reaction path, including of course the saddle point geometry.

As a first step in the validation of the new approach, we have performed two critical tests. In one we tested /// direct dynamics against straight direct dynamics for the reaction CF_3 + $HCD_3 \rightarrow CF_3$ H + CD_3 [49c]. This reaction was chosen because it is dominated by large-curvature tunneling [17], and so it tests the most difficult part of the correction algorithm. In this case we used our 6-parameter NDDO-SRP implicit potential energy function [17], based on changing six parameters of the general AM1 [45b,45c] parameterization of NDDO theory, as the high level of theory, and we created a purposely very inaccurate surface to serve as the low level in order to provide a severe test. The test was carried out by comparing a straight direct dynamics calculation at the high level to another calculation in which we assumed that we know the high level results through the hessian expansion at four stationary points (reactants, well between reactants and saddle point, saddle point itself, and well between saddle point and products) and used these results to "correct" the low-level calculation. For the low level, we varied only one parameter in the MNDO [45a] general parameterization of NDDO theory in order to make

the exoergicity right (0.7 kcal exoergic). This yields a barrier height that is 6.6 kcal too high (21.2 kcal vs. the "high-level" 14.6). It is *very easy* to get a better low-level surface, but that was not our goal here. Rather this is designed to be a difficult test for dual-level direct dynamics. Table 2 shows some of the results [49c]. At 350 K, a straight direct dynamics calculation predicts a rate constant larger than conventional TST at 350 K by a factor of about 20. The table shows that we can get a factor of about 15 by using the high-level results through a hessian expansion about only four stationary points. The actual ratios computed using more significant figures than shown in Table 2 yield factors of 20 and 13, respectively, a discrepancy of 35%. This discrepancy is reduced to 15% at 400 K and to an average value of 28% at 600–1500 K. For $CF_3 + CD_3H \rightarrow CF_3D + CD_2H$, the average error from 350 K to 1500 K is only 25%. Recalling that the low-level calculation used was designed to provide a difficult test, the results are satisfactory.

A second test was carried out for the reaction $OH + CH_4 \rightarrow H_2O + CH_3$ [49c]. Results obtained at several levels for this reaction are shown in Table 3. The original AM1 parameters yield a barrier height of 11.1 kcal/mol and an exoergicity of 21.1. The cc-pVTZ basis set of Dunning [58] was adjusted to yield the correct (experimental) exoergicity of 13.3 kcal/mol at the MP2-SAC [43b] level; this calculation then predicts a barrier height of 7.4 kcal/mol and a conventional TST rate constant at 350 K of 0.4 ×

Table 2. Rate constants (10^{-20} cm^3 $molecule^{-1}$ s^{-1}) calculated by conventional and variational transition state theory for $CF_3 + CHD_3 \rightarrow CF_3H + CD_3$.

Potential surface				Dynamical level	T (K)	k(T)
High level	Low level	Approach	HL points			
AM2-SRP(6)[a]	· · ·	conventional	2	TST	350	0.2
					400	2
AM1-SRP(6)	· · ·	single-level	600	CVT/μOMT	350	4
					400	20
MNDO-SRP(1)	· · ·	"	600	CVT/μOMT	350	0.0003
					400	0.004
AM1-SRP(6)	MNDO-SRP(1)	dual-level	4	CVT/μOMT	350	3
					400	17

[a]Number in parentheses is number of SRP parameters.

Table 3. Rate constants (10^{-14} $cm^3 molecule^{-1} s^{-1}$) calculated by various approaches and with various sources of potential data for the reaction $OH + CH_4 \rightarrow H_2O + CD_3$.

Potential surface				Dynamical level	k (T = 350 K)
High level	Low level	Approach	HL points		
AM1-SRP[a]	. . .	conventional	2[b]	TST	1.1
AM1-SRP	. . .	VTST	210	CVT/μOMT	0.9
MP2-SAC/cc-pVTZ[c]	. . .	conventional	2[b]	TST	0.4
"	. . .	IVTST	3	CVT/SCT	2.0
"	. . .	"	5	CVT/SCT	1.1
"	AM1-SRP	VTST-IC	3	CVT/SCT	1.1
"	"	"	3	CVT/μOMT	1.1
				Experiment	1.6

[a]two parameters reoptimized
[b]reactant and saddle point only
[c]basis adjusted for correlation balance as explained in Ref. [18]

10^{-14} $cm^3 molecule^{-1} s^{-1}$. Using the reactant and saddle point properties required for this calculation plus a calculation at the product geometry (which was needed to adjust the basis set to predict the correct exoergicity) along with the IVTST method raises the predicted rate constant to 2.0×10^{-14} kcal/mol, and adding two more MP2-SAC points lowers this to 1.1×10^{-14} [18]. Recall that the IVTST method, at least as currently formulated, cannot treat large-curvature tunneling so these results are based on the SCT approximation. The estimation of the reaction-path curvature throughout the whole region that is important for tunneling on the basis of only three points in the vicinity of the saddle point is the least trustworthy part of this calculation.

Repeating this calculation at the VTST-IC level (/// dynamics) allows us to make a more reliable estimate of the reaction-path curvature and of the shapes of the various generalized transition state theory frequencies as well as to include large-curvature tunneling. Thus we adjusted the AM1 parameters to reproduce the MP2-SAC barrier height and the experimental exoergicity, and we used this surface as a low-level surface for the dual-level VTST-IC approach [49c]. Table 3 shows that, even using the results of the MP2-SAC calculation for only 3 points (reactant, saddle point, and product) yields a rate constant of 1.1×10^{-14}, in excellent agreement with the IVTST level.

The first application of the VTST-IC method to a new problem was to the reaction $OH + NH_3 \rightarrow H_2O + NH_2$ [49d]. In this case we used two different low-level theories.

The first low-level theory is an NDDO-SRP calculation in which the functional form of the PM3 version of NDDO theory was generalized to allow a larger number of resonance integral parameters. In the original AM1 and PM3 parameterizations, there are five resonance parameters for a system composed of H, C, and N, namely β_{Hs}, β_{Cs}, β_{Cp}, β_{Ns}, and β_{Np}. Resonance parameters $\beta_{X\ell X'\ell'}$ for the interaction of an ℓ-type orbital on atom X with an ℓ'-type orbital on atom X are then approximated by

$$\beta_{X\ell X'\ell'} = \frac{\beta_{X\ell} + \beta_{X'\ell'}}{2} \tag{18}$$

In our treatment we took all nine unique pairs (only nine because there are no O-O or N-N pairs in the $OH + NH_3$ system) of $X\ell$ and $X'\ell'$ as independent. The values of β_{HsHs}, β_{NsOs}, β_{NsOp}, and β_{NpOs} were kept the same as in PM3 (based on eq. 8 with PM3 values for the β_{Xl}), but we independently re-optimized β_{HsNs}, β_{HsNp}, β_{HsOs}, β_{HsOp}, and β_{NpOp}.

For the alternative low level, we used an *ab initio* direct dynamics calculation at the MP2/6-31G** [42] level.

For the high level we used the MP2/aug-cc-pVTZ level for stationary point optimizations, the QCISD(T)/aug-cc-pVTZ level for single point calculations of the energy at the resulting optimized geometries, and the MP2/aug-cc-pVDZ level for hessians at the corresponding stationary points. (The notation for correlation levels and basis sets is standard [42,578,59].)

Table 4 compares the calculated barrier heights at various levels of theory. This table clearly illustrates the advantages of dual-level and interpolatory techniques in that very large basis sets and high levels of treating electron correlation are required to obtain an accurate barrier height. If one were forced to use such a computationally demanding electronic structure calculations for all steps of the dynamics calculation, direct dynamics without interpolation would be impractical, whereas if one restricted oneself to the more affordable lower level, the barrier and frequencies would not be nearly as accurate as in the dual-level calculation.

Figure 1 compares the profile of the most strongly varying generalized normal mode frequency as calculated four different ways. The frequency shown in Figure 1 correlates with N–H stretching in the reactants and with O–H stretching in the products. This curve shows a shape very characteristic of atom-transfer reactions in general, in that it is typical for the frequency associated with the breaking bond to decrease rapidly when the bond switching occurs in the strong interaction region, where there are two half bonds, and then to increase as the associated vibrational mode transforms itself into a product stretch [8k,81,35,60]. Interpolation of this bond-switching-mode frequency is very challenging

because of its rapidly varying character, but it is critical to capture this variation because it is a high-frequency mode, and high-frequency modes carry a considerable amount of zero point energy. (For example, the difference in zero point energy between a 1500 cm^{-1} mode in the bond-switching region and a 3500 cm^{-1} mode in the reactant region is 2.9 kcal/mol, and even the difference in zero point energy between a 1500 cm^{-1} mode and a 2000 cm^{-1} mode at two different points in the bond-switching region is 0.7 kcal/mol.) Figure 1 shows that the two corrected calculations give identical frequencies at $s = 0$, as they should since they are both corrected to the same high level at this point, but the reactive mode profile differs elsewhere because of differences between the two low-level calculations. The s value around which the minimum of the bond-switching-mode frequency tends to be centered depends strongly on the geometry of the saddle point, and this is a primary reason why it is important for the low-level calculation to yield a reasonably accurate saddle point geometry. Since saddle point geometry tends to correlate with reaction exoergicity [37a,61], we believe it is important for the low-level calculation to have the correct (or close to the correct) exoergicity, and this is one reason that we have emphasized the exoergicity in deriving SRP parameters. Figure 1 also illustrates the advantage of VTST-IC over IVTST, namely that reasonable low-level surfaces are excellent *chemical* interpolators because they have the chemical variation of the frequencies "built in." Thus dual-level approaches yield more accurate vibrational profiles than interpolations based on *mathematically* motivated forms.

Table 5 gives calculated rate constants with the chosen higher level and the alternative lower levels. Table 5 shows excellent agreement between calculations carried out with the two very different lower levels, up through CVT/SCT dynamics. It would be very expensive to calculate large-curvature tunneling with an *ab initio* lower level, but here the dual-level approaches with an NDDO-SRP lower level really prove their mettle. Large-curvature effects increase the calculated rate constant by a factor of 2.0 at 250 K, bringing the result into excellent agreement with experiment. The agreement with experiment for

Table 4. Number of basis functions and calculated barrier height (kcal/mol) for $OH + NH_3 \rightarrow H_2O + NH_2$ at various levels of electronic structure theory.

Level	Number	$V^{\neq}$
PM3	12	13.7
PM3-SRP	12	5.9
MP2/6-31G**	50	9.0
MP2/aug-cc-pVDZ	82	5.8
MP2/aug-cc-pVTZ	184	4.5
QCISD(T)/aug-cc-pVTZ//MP2	184	3.6

[a]X/Y//X′ means a single-point energy calculated at level X/Y at a geometry optimized at level X′/Y.

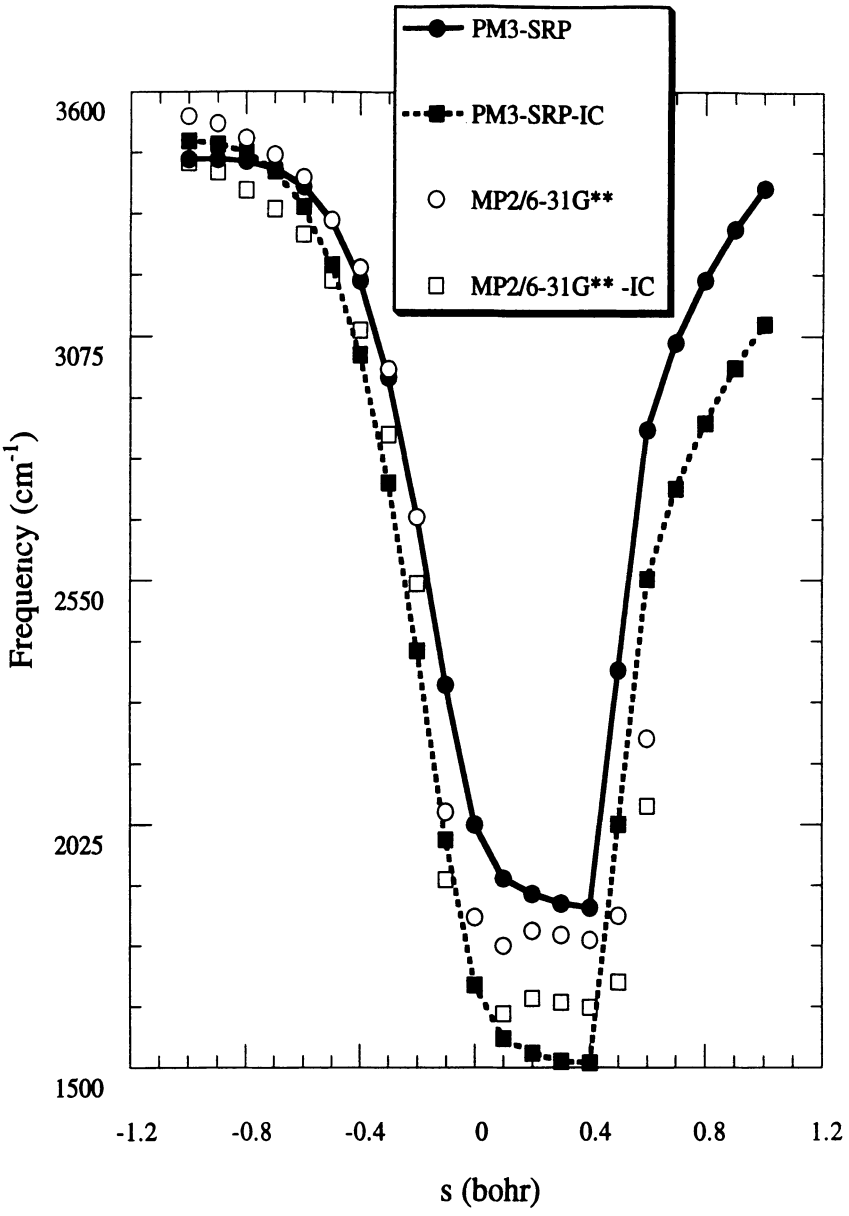

Figure 1. The generalized-normal-mode frequency for the bond-switching mode as a function of reaction coordinate for $OH + NH_3 \rightarrow H_2O + NH_2$.

the OH + NH_3 reaction is especially impressive because of the large Arrhenius curvature. Table 6 gives Arrhenius activation energies over three temperature ranges showing the dramatic lowering at low temperature.

Further improvements in these methods should allow a wide variety of interesting processes to be studied.

Table 5. Calculated VTST-IC rate constants (10^{-13} cm^3 $molecule^{-1}$ s^{-1}) at the QCISD(T)/aug-cc-pVTZ//MP2[MP2/aug-cc-pVDZ]///LL level of electronic structure theory.[a]

Dynamical level	T (K)	LL	
		MP2/6-31G**	NDDO-SRP
TST	250	0.18	0.18
	300	0.42	0.42
	1000	25	25
CVT/SCT	250	0.66	0.68
	300	1.03	1.06
	1000	26	25
CVT/μOMT	250	. . .	1.36
	300	. . .	1.69
	1000	. . .	26
Experiment	250	1.2	1.2
	300	2.0	2.0
	1000	31	31

[a]HL[HessL]///LL denotes a higher level of HL, except for the hessians which are calculated at level HessL, and a lower level of LL in a dual-level direct dynamics calculation.

Table 6. Arrhenius activation energies from fits to calculated rate constants at pairs of temperatures in the low, middle, and high-temperature regimes, based on NDDO-SRP as the low level and CVT/μOMT dynamics.

Temperature interval (K)	E_a (kcal/mol)
250–300	0.65
400–600	2.1
800–1000	4.6

4. Vibrational coordinates

Another area where technical advances are in progress is the treatment of the vibrations perpendicular to the reaction path. A central assumption of all reaction-path methods, including variational transition state theory and small-curvature tunneling methods, is the separation of the coordinates into three sets: external coordinates describing the overall translation and rotation, a reaction coordinate describing the motion of the system along some direct route from reactants to products, and the remaining coordinates, which will be called the bound vibrational coordinates.

For linear displacements from a stationary point, separable coordinates are uniquely defined for small displacements by normal mode coordinates [62], which simultaneously diagonalize the kinetic energy to infinite order and the potential energy to second order (i.e., through quadratic terms in the potential). Thus, to the extent that one stays in a region where the quadratic expansion of the potential is trustworthy, these coordinates separate the physical motion, and they are not just an artificial mathematical imposition. Not only is the motion separable in normal coordinates, but the coordinates themselves are very convenient for calculations, since they are rectilinear.

Such comfortingly natural and convenient coordinates do not exist though if we add the requirement that one of the coordinates describes the global motion of the system along some direct route from reactants to products. In general this cannot be accomplished in a convenient way with rectilinear coordinates, and one must introduce at least one curvilinear coordinate. The basic formalism for such a treatment was first advanced in the context of the large-amplitude vibrational motion of small molecules by various workers [63] and in the context of bimolecular reactions by Hofacker [20b], Marcus [12b,12c,20c,22], and others (for an extensive set of references, see Refs. 1–34 in [31a]). The approach used for large-amplitude vibrational motion was further developed for the case where the large-amplitude "coordinate" is the minimum energy path by Miller *et al.* [34] and by Natanson [64]. In these approaches, the reaction coordinate is curvilinear but the coordinates transverse to the reaction path are Cartesian. Hence we call this kind of treatment the Cartesian vibration (CV) approximation.

For variational transition state theory, one requires the vibrational Hamiltonian only in a hypersurface perpendicular to the reaction coordinate. For such calculations the global CV treatments for chemical reactions reduce to an earlier method [8j] in which a local Cartesian system is erected at a point on the MEP, with one of the axes aligned with the tangent to the path. However, for reaction-path-based tunneling calculations, one must consider the globally curved nature of reaction coordinate.

Both for VTST and for tunneling calculations, though, the CV coordinate system is often unsatisfactory, for two reasons. The first problem is that it has the same disadvantages as rectilinear coordinates for vibrational calculations on bound systems—in particular it does not provide a physically natural picture of valence forces, and so there are large

anharmonic cross terms [65]. This problem is discussed elsewhere in the context of reaction-path dynamics [66]. Although this problem is serious in both bound-state theory (spectroscopy) and reaction-path dynamics, an even more serious problem occurs in the latter because even the harmonic frequencies are not independent of the coordinate system used for the generalized normal mode analysis at a non-stationary point [31,64]. As a consequence the generalized normal mode frequencies may become unphysically imaginary (as if the reaction path were a ridge) even when the reaction path sits at the bottom of a nonbifurcating valley [31a,67]. This happens frequently in the CV treatment because the Cartesian vibrational coordinates are nonphysical.

A better approach to modeling the vibrations transverse to the reaction path is to use curvilinear vibrational coordinates based on bond stretches, valence angle bends, bbond torsions (defined by dihedral angle between the ABC plane and the BCD plane in a group of atoms with the sequential bonding pattern A–B–C–D), and sometimes "improper dihedrals" (the angle between a bond and a plane). These curvilinear coordinates should provide a better description of generalized transition state vibrations for the same reasons that they are preferable to rectilinear coordinates for treating vibrations of bound molecules, namely that they tend to follow natural contours of the potential energy surface. Techniques for treating the transverse vibrations in curvilinear coordinates have been developed [31] and should be very useful for future work.

5. Summary

This chapter provides an account of our recent efforts to interface dynamics calculations based on reaction-path potentials and tunneling, including tunneling through the large-curvature reaction swath, with electronic structure theory.

6. Acknowledgments

I am grateful to Kim Baldridge, Jose C. Corchado, Joaquin Espinosa-Garcia, Bruce C. Garrett, Angels Gonzalez-Lafont, Mark S. Gordon, Michael Gu, Wei-Ping Hu, Charles Jackels, Yi-Ping Liu, Da-hong Lu, Gillian C. Lynch, Vasilios Melissas, Grigory Natanson, Kiet Nguyen, Ivan Rossi, Rozeanne Steckler, and Thanh Truong for their collaboration on the development and implementation of direct dynamics and internal coordinates techniques for chemical kinetics. The author's research on variational transition state theory and semiclassical tunneling method is supported by the U.S. Department of Energy, Office of Basic Energy Sciences. The author's research on high-energy chemical reactions is supported by NASA.

References

[1] (a) D. G. Truhlar, D. W. Schwenke, and D. J. Kouri, J. Phys. Chem. **94**, 7346 (1990). (b) D. E. Manolopoulos and R. E. Wyatt, J. Chem. Phys. **92**, 810 (1990). (c) W. H. Miller, Annu. Rev. Phys. Chem. **41**, 245 (1991). (d) J. M.

Launay, Theor. Chim. Acta **79**, 183 (1991). (e) R. T Pack, E. A. Butcher, and G. A. Parker, J. Chem. Phys. **99**, 9310 (1993).

[2] S. L. Mielke, G. C. Lynch, D. G. Truhlar, and D. W. Schwenke, J. Phys. Chem. **98**, 8000 (1994).

[3] A. J. C. Varandas, F. B. Brown, C. A. Mead, D. G. Truhlar, and N. C. Blais, J. Chem. Phys. **86**, 6258 (1987).

[4] J. V. Michael and J. R. Fisher, J. Phys. Chem. **94**, 3318 (1990).

[5] B. C. Garrett, D. G. Truhlar, A. J. C. Varandas, and N. C. Blais, Int. J. Chem. Kinet. **18**, 1065 (1986).

[6] (a) M. M. Kreevoy and D. G. Truhlar, in Investigation of Rates and Mechanisms of Reaction, 4th edition, C. F. Bernasconi (ed.), John Wiley & Sons, New York, 1986, Pt. I, p. 13. (b) D. G. Truhlar and B. C. Garrett, J. Chim. Phys. **84**, 365 (1987). (c) S. C. Tucker and D. G. Truhlar, in New Theoretical Concepts for Understanding Organic Reactions, J. Bertrán and I. G. Csizmadia (eds.), Kluwer, Dordrecht, 1989, p. 291.

[7] (a) S. C. Tucker and D. G. Truhlar, J. Amer. Chem. Soc. **112**, 3347 (1990). (b) Y.-P. Liu, G. C. Lynch, T. N. Truong, D.-h. Lu, D. G. Truhlar, and B. C. Garrett, J. Amer. Chem. Soc. **115**, 2408 (1993). (c) S. E. Wonchoba and D. G. Truhlar, J. Chem. Phys. **99**, 9637 (1993). (d) V. S. Melissas and D. G. Truhlar, J. Phys. Chem. **98**, 875 (1994).

[8] (a) E. Wigner, J. Chem. Phys. **5**, 720 (1937). (b) J. Horiuti, Bull. Chem. Soc. Japan **13**, 210 (1938). (c) M. A. Eliason and J. O. Hirschfelder, J. Chem. Phys. **30**, 1426 (1959). (d) J. C. Keck, J. Chem. Phys. **32**, 1035 (1960). (e) J. C. Keck, Advan. Chem. Phys. **13**, 85 (1967). (f) D. G. Truhlar, J. Chem. Phys. **53**, 2041 (1970). (g) A. Tweedale and K. J. Laidler, J. Chem. Phys. **53**, 2045 (1970). (h) G. W. Koeppl, J. Amer. Chem. Soc. **96**, 6539 (1974). (i) W. H. Miller, J. Chem. Phys. **61**, 1823 (1974). (j) B. C. Garrett and D. G .Truhlar, J. Chem. Phys. **70**, 1593 (1979). (k) B. C. Garrett and D. G. Truhlar, J. Phys. Chem. **83**, 1052 (1979). (l) B. C. Garrett and D. G. Truhlar, J. Phys. Chem. **83**, 1079 (1979).

[9] (a) S. Glasstone, K. Laidler, and H. Eyring, The Theory of Rate Processes, McGraw-Hill, New York 1941. (b) K. J. Laidler, Chemical Kinetics, 3rd ed., Harper & Row, New York, 1987.

[10] D. G. Truhlar, A. D. Isaacson, and B. C. Garrett, in Theory of Chemical Reaction Dynamics, M. Baer (ed.), CRC Press, Boca Raton, 1985, Vol. 4, p. 65.

[11] D. G. Truhlar and B. C. Garrett, Accounts Chem. Res. **13**, 440 (1980).

[12] (a) I. Shavitt, J. Chem. Phys. **49**, 4048 (1968). (b) R. A. Marcus, J. Chem. Phys. **45**, 4493 (1966). (c) R. A. Marcus, J. Chem. Phys. **49**, 2610 (1968). (d) D. G. Truhlar and A. Kuppermann, J. Amer. Chem. Soc. **93**, 1840 (1970). (e) D. G. Truhlar and A. Kuppermann, J. Chem. Phys. **56**, 2232 (1972). (f) K. Fukui, in The World of Quantum Chemistry, R. Daudel and B Pullman (eds.), Reidel, Dordrecht, 1974, p. 113.

[13] H. Eyring, J. Chem. Phys. **3**, 107 (1935).

[14] E. P. Wigner, Z. Phys. Chem., Abt. B **19**, 203 (1932).

[15] (a) D. C. Chatfield, R. S. Friedman, D. G. Truhlar, B. C. Garrett, and D. W. Schwenke, J. Amer. Chem. Soc. **113**, 486 (1991). (b) D. C. Chatfield, R. S. Friedman, D. G. Truhlar, and D. W. Schwenke, Faraday Discussions Chem. Soc. **91**, 289 (1991). (c) D. C. Chatfield, R. S. Friedman, G. C. Lynch, D. G. Truhlar, and D. W. Schwenke, J. Chem. Phys. **98**, 342 (1993). (d) D. C. Chatfield, R. S. Friedman, D. W. Schwenke, and D. G. Truhlar, J. Phys. Chem. **96**, 2414 (1992).

[16] B. C. Garrett and D. G. Truhlar, Proc. Natl. Acad. Sci. USA **76**, 4755 (1979).

[17] Y.-P. Liu, D.-h. Lu, A. Gonzalez-Lafont, D. G. Truhlar, and B. C. Garrett, J. Amer. Chem. Soc. **115**, 7806 (1993).

[18] V. S. Melissas and D. G. Truhlar, J. Chem. Phys. **99**, 1013 (1993).

[19] (a) R. T. Skodje, D. G. Truhlar, and B. C. Garrett, J. Chem. Phys. **77**, 5955 (1982). (b) B. C. Garrett, D. G. Truhlar, A. F. Wagner, and T. H. Dunning, Jr., J. Chem. Phys. **76**, 1380 (1982). (c) B. C. Garrett and D. G. Truhlar, J. Chem. Phys. **81**, 309 (1984). (d) B. C. Garrett, N. Abusalbi, D. J. Kouri, and D. G. Truhlar, J. Chem. Phys. **83**, 2252 (1985). (e) B. C. Garrett, D. G. Truhlar, and G. C. Schatz, J. Amer. Chem. Soc. **108**, 2876 (1986). (f) G. C. Lynch, D. G. Truhlar, and B. C. Garrett, J. Chem. Phys. **90**, 3102 (1989); erratum: **91**, 3280 (1989). (g) B. C. Garrett, T. Joseph, T. N. Truong, and D. G. Truhlar, Chem. Phys. **136**, 271 (1989); erratum: **140**, 207 (1990). (h) D. G. Truhlar, J. Chem. Soc. Faraday Trans. **90**, 1740 (1994).

[20] (a) M. A. Eliason and J. O. Hirschfelder, J. Chem. Phys. **30**, 1426 (1959). (b) L. Hofacker, Z. Naturforsch. **18a**, 607 (1963). (c) R. A. Marcus, Discussions Faraday Soc. **44**, 7 (1967). (d) D. G. Truhlar, J. Chem. Phys. **53**, 2041 (1970). (e) B. C. Garrett, D. G. Truhlar, R. S. Grev, and A. W. Magnuson, J. Phys. Chem. **84**, 1730 (1984).

[21] G. C. Lynch, P. Halvick, D. G. Truhlar, B. C. Garrett, D. W. Schwenke, and D. J. Kouri, Z. Naturforsch. **44a**, 427 (1989).

[22] R. A. Marcus, J. Chem. Phys. **49**, 2617 (1969).

[23] R. A. Marcus and M. E. Coltrin, J. Chem. Phys. **67**, 2609 (1977).

[24] D.-h. Lu, T. N. Truong, V. S. Melissas, G. C. Lynch, Y.-P. Liu, B. C. Garrett, R. Steckler, A. D. Isaacson, S. N. Rai, G. C. Hancock, J. G. Lauderdale, T. Joseph, and D. G. Truhlar, Computer Phys. Commun. **71**, 235 (1992).

[25] T. N. Truong, D.-h. Lu, G. C. Lynch, Y.-P. Liu, V. S. Melissas, J. J. P. Stewart, R. Steckler, B. C. Garrett, A. D. Isaacson, A. Gonzalez-Lafont, S. N. Rai, G. C. Hancock, T. Joseph, and D. G. Truhlar, Computer Phys. Commun. **75**, 143 (1993).

[26] B. C. Garrett and D. G. Truhlar, J. Chem. Phys. **79**, 4931 (1983).

[27] B. C. Garrett and D. G. Truhlar, J. Phys. Chem. **83**, 2921 (1979).

[28] A. D. Isaacson and D. G. Truhlar, J. Chem. Phys. **76**, 1380 (1982).

[29] A. D. Isaacson, M. T. Sund, S. N. Rai, and D. G. Truhlar, J. Chem. Phys. **82**, 1338 (1985).

[30] (a) D. G. Truhlar and A. D. Isaacson, J. Chem. Phys. **77**, 3516 (1982). (b) B. C. Garrett and D. G. Truhlar, J. Phys. Chem. **89**, 2204 (1985). (c) B. C. Garrett, N. Abusalbi, D. J. Kouri, and D. G. Truhlar, J. Chem. Phys. **83**, 2252 (1985). (d) B. C. Garrett and D. G. Truhlar, Int. J. Quantum Chem. **29**, 1463 (1986). (e) R. Steckler, D. G. Truhlar, and B. C. Garrett, J. Chem. Phys. **84**, 6712 (1986). (f) B. C. Garrett, D. G. Truhlar, A. J. C. Varandas, and N. C. Blais, Int. J. Chem. Kinet. **18**, 1065 (1986). (g) B. C. Garrett, D. G. Truhlar, J. M. Bowman, and A. F. Wagner, J. Phys. Chem. **90**, 4305 (1986). (h) J. Z. H. Zhang, Y. Zhang, D. J. Kouri, B. C. Garrett, K. Haug, D. W. Schwenke, and D. G. Truhlar, Faraday Discussions Chem. Soc. **84**, 371 (1987).

[31] (a) G. A. Natanson, B. C. Garrett, T. N. Truong, T. Joseph, and D. G. Truhlar, J. Chem. Phys. **94**, 7875 (1991). (b) C. F. Jackels, M. Z. Gu, and D. G. Truhlar, J. Chem. Phys., in press.

[32] (a) K. Ishida, K. Morokuma, and A. Komornicki, J. Chem. Phys. **66**, 2153 (1977). (b) M. W. Schmidt, M. S. Gordon, and M. J. Dupuis, J. Amer. Chem. Soc. **107**, 2585 (1985). (c) B. C. Garrett, M. J. Redmon, R. Steckler, D. G. Truhlar, K. K. Baldridge, D. Bartel, M. W. Schmidt, and M. S. Gordon, J.

Phys. Chem. **92**, 1476 (1988). (d) K. K. Baldridge, M. S. Gordon, R. Steckler, and D. G. Truhlar, J. Phys. Chem. **93**, 5107 (1989). (e) V. S. Melissas, D. G. Truhlar, and B. C. Garrett, J. Chem. Phys. **96**, 5758 (1992).

[33] (a) M. Page and J. W. McIver, Jr., J. Chem. Phys. **88**, 992 (1988). (b) C. Gonzalez and H. B. Schlegel, J. Phys. Chem. **94**, 5523 (1990). (c) J.-Q. Sun and K. Ruedenberg, J. Chem. Phys. **99**, 5257 (1993).

[34] W. H. Miller, N. C. Handy, and J. E. Adams, J. Chem. Phys. **72**, 99 (1980).

[35] (a) B. C. Garrett and D. G. Truhlar, J. Amer. Chem. Soc. **101**, 4534 (1979). (b) B. C. Garrett and D. G. Truhlar, J. Amer. Chem. Soc. **101**, 5207 (1979).

[36] D. G. Truhlar, J. Comp. Chem. **12**, 266 (1991).

[37] (a) C. A. Parr and D. G. Truhlar, J. Phys. Chem. **75**, 1844 (1971). (b) D. G. Truhlar and R. E. Wyatt, Adv. Chem. Phys. **36**, 141 (1977). (c) W. L. Hase and R. J. Wolf, in Potential Energy Surfaces and Dynamics Calculations, D. G. Truhlar (ed.), Plenum, New York, 1981, p. 37. (d) D. G. Truhlar, R. Steckler, and M. S. Gordon, Chem. Rev. **87**, 217 (1987). (e) G. C. Schatz, Rev. Mod. Phys. **61**, 669 (1989).

[38] T. Joseph, R. Steckler, and D. G. Truhlar, J. Chem. Phys. **87**, 7036 (1987).

[39] S. C. Tucker and D. G. Truhlar, J. Amer. Chem. Soc. **112**, 3338 (1990).

[40] S. L. Mielke, G. C. Lynch, D. G. Truhlar, and D. W. Schwenke, Chem. Phys. Lett. **213**, 10 (1993); erratum: **217**, 173 (1994).

[41] (a) G. C. Lynch, D. G. Truhlar, F. B. Brown, and J.-g. Zhao, Hyperfine Interactions **87**, 885 (1984). (b) G. C. Lynch, D. G. Truhlar, F. B. Brown, and J.-g. Zhao, J. Phys. Chem. **99**, 207 (1995).

[42] W. J. Hehre, L. Radom, P. v. R. Schleyer, and J. A. Pople, Ab Initio Molecular Orbital Theory, Wiley, New York, 1986.

[43] (a) F. B. Brown and D. G. Truhlar, Chem. Phys. Lett. **117**, 307 (1985). (b) M. S. Gordon and D. G. Truhlar, J. Amer. Chem. Soc. **108**, 542 (1986).

[44] (a) W. Kohn and L. Sham, Phys. Rev. A **140**, 1133 (1955). (b) W. A. Harrison, Electronic Structure and the Properties of Solids, Freeman, San Francisco, 1980. (c) D. Tomańek and M. A. Schluter, Phys. Rev. B **36**, 1208 (1987). (d) T. Ziegler, Chem. Rev. **91** (1991) 651.

[45] (a) M. J. S. Dewar and W. Thiel, J. Amer. Chem. Soc. **99**, 4899, 4907 (1977). (b) M. J. S. Dewar, E. G. Zoebisch, E. F. Healy, and J. J. P. Stewart, J. Amer. Chem. Soc. **107**, 3902 (1985). (c) M. J. S. Dewar and E. G. Zoebisch, Theochem **180**, 1 (1988). (d) J. J. P. Stewart, J. Comp. Chem. **10**, 221 (1989). (e) J. J. P. Stewart, J. Computer-Aided Mol. Design **4**, 1 (1990).

[46] (a) I. Wang and M. Karplus, J. Amer. Chem. Soc. **95**, 8160 (1973). (b) D. J. Malcome-Lawes, J. Chem. Soc. Faraday Trans. II **71**, 1183 (1975). (c) C. Leforestier, J. Chem. Phys. **68**, 4406 (1978).

[47] (a) R. Car and M. Parrinello, Phys. Rev. Lett. **55**, 2471 (1985). (b) O. F. Sankey and R. E. Allen, Phys. Rev. B **33**, 7164 (1986). (c) M. R. Pederson, B. M. Klein, and J. Q. Broughton, Phys. Rev. B **38**, 3825 (1988). (d) C. Z. Wang, C. T. Chen, and K. M. Ho, Phys. Rev. B **39**, 8586 (1989). (e) O. F. Sankey and D. J. Niklewski, Phys. Rev. B **40**, 3979 (1989). (f) J. Harris and D. Hohl, J. Phys.: Condens. Matter **2**, 5161 (1990). (g) D. A. Drabold, P. A. Fedders, O. F. Sankey, and J. O. Dow, Phys. Rev. B **42**, 5135 (1990). (h) G. Galli and M. Parrinello, in Computer Simulations in Materials Science, M. Meyer and V. Pontikis (eds.), Kluwer, Dordrecht, 1991, p. 283. (i) R. N. Barnett, U. Landman, A. Nitzan, and G. Rajagopal, J. Chem. Phys. **94**, 608 (1991). (j) R. M. Wentzcovitch and J. L. Martins, Solid State Commun. **78**, 831 (1991). (k) F. S. Khan and J. Q. Broughton, Phys. Rev. B **43**, 11754 (1991). (l) M. C. Payne, M. P. Teter, D. C. Allen, T. A. Arias, and J. D. Joannopoulos, Rev. Mod. Phys. **64**, 1045 (1992). (m) B. Hartke and E. A. Carter, Chem. Phys. Lett. **189**, 358 (1992). (n) R. M. Wentzcovitch, J. L. Martins, and G. D. Price, Phys. Rev. Lett. **70**, 3947 (1993). (o) D. A. Gibson and E. A. Carter, J. Phys. Chem. **97**, 13429 (1993). (p) R. N. Barnett and U. Landman, Phys. Rev. B **48**, 2081 (1993). (q) M. J. Field, in Computer Simulations of Biomolecular Systems, Vol. 2, W. F. Van Gunsteren, P. K. Weiner, and A. J. Wilkonson (eds.), ESCOM, Leiden, 1993, p. 82. (r) D. L. Lynch, N. Troullier, J. D. Kress, and L. A. Collins, J. Chem. Phys. **101**, 7048 (1994). (s) W. Chen. W. L. Hase, and H. B. Schlegel, Chem. Phys. Lett. **228**, 436 (1994). (t) C. Lee, X. Long, I. Carpenter, S. Smithline, and G. Fitzgerald, Int. J. Quantum Chem. **47**, 527 (1994).

[48] (a) A. Warshel and M. Karplus, Chem. Phys. Lett. **32**, 11 (1975). (b) D. G. Truhlar, J. W. Duff, N. C. Blais, J. C. Tully, and B. C. Garrett, J. Chem. Phys. **77**, 764 (1982).

[49] (a) A. Gonzalez-Lafont, T. N. Truong, and D. G. Truhlar, J. Phys. Chem. **95**, 4618 (1991). (b) A. A. Viggiano, J. Paschkewitz, R A. Morris, J. F. Paulson, A. Gonzalez-Lafont, and D. G. Truhlar, J. Amer. Chem. Soc. **113**, 9404 (1991). (c) W.-P. Hu, Y.-P. Liu, and D. G. Truhlar, J. Chem. Soc. Faraday Trans. **90**, 1715 (1994). (d) J. C. Corchado, J. Espinosa-García, W.-P. Hu, I. Rossi, and

D. G. Truhlar, J. Phys. Chem. **99**, 687 (1995). (e) W.-P. Hu, I. Rossi, and D. G. Truhlar, work in progress.

[50] (a) A. Tachibana, I. Ukazaki, M. Koizumi, K. Hori, and T. Yomabe, J. Amer. Chem. Soc. **107**, 1190 (1985). (b) S. M. Colwell and N. C. Handy, J. Chem. Phys. **82**, 1281 (1985). (c) C. Doubleday, Jr., J. W. McIver, Jr., and M. Page, J. Phys. Chem. **92**, 4367 (1988). (d) B. C. Garrett, M. L. Koszykowski, C. F. Melius, and M. Page, J. Phys. Chem. **94**, 7096 (1990). (e) T. N. Truong and J. A. McCammon, J. Amer. Chem. Soc. **113**, 7504 (1991). (f) B. C. Garrett and C. F. Melius, in Theoretical and Computational Models for Organic Chemistry, S. J. Formosinho, I. G. Csizmadia, and L. G. Arnaut (eds.), Kluwer, Dordrecht, 1991, p. 35. (g) J. W. Storer and K. N. Houk, J. Amer. Chem. Soc. **115**, 10426 (1993). (h) T. N. Truong, J. Chem. Phys. **100**, 8014 (1993). (i) J. Espinosa-García and J. C. Corchado, J. Chem. Phys. **101**, 1333 (1994). (j) T. N. Truong and W. Duncan, J. Chem. Phys. **101**, 7408 (1994). (k) J. Espinosa-García and J. C. Corchado, J. Chem. Phys. **101**, 8700 (1994). (l) T. N. Truong and T. J. Evans, J. Chem. Phys. to be published. (m) R. L. Bell and T. N. Truong, J. Chem. Phys., to be published.

[51] (a) D. G. Truhlar and M. S. Gordon, Science **249**, 491 (1990). (b) M. Page, Computer Phys. Commun. **84**, 115 (1994).

[52] I. Rossi and D. G. Truhlar, Chem. Phys. Lett. **233**, 231 (1995).

[53] (a) D. E. Goldberg, Genetic Algorithms in Search, Optimization, and Machine Learning, Addison-Wesley, Reading, MA, 1989. (b) J. H. Holland, Scientific American, July, 1992, p. 66. (c) E. J. Anderson and M. J. Ferris, in Parallel Processing for Scientific Computing, J. Dongarra, P. Messina, D. C. Sorensen, and R. G. Voigt (eds.), SIAM, Philadelphia, 1989, p. 137. (d) T. Bäck and F. Hoffmeister, in Proceedings of the Fourth International Conference on Genetic Algorithms, R. K. Belew and L. B. Booker (eds.), Morgan Kaufmann, San Mateo, CA, 1991, p. 92. (e) R. S. Judson, E. P. Jaeger, A. M. Treasurywala, and M. L. Peterson, J. Comp. Chem. **14**, 1407 (1993). (f) D. B. McGarrah and R. S. Judson, J. Comp. Chem. **14**, 1385 (1993). (g) Y. L. Xiao and D. E. Williams, J. Phys. Chem. **98**, 7191 (1994).

[54] (a) T. Bäck, F. Hoffmeister, and H.-P. Schwefel, in Proceedings of the Fourth International Conference on Genetic Algorithms, R. K. Belew and L. B. Booker (eds.), Morgan Kaufmann, San Mateo, CA, 1991, p. 2. (b) J. J. Grefenstette, in Proceedings of the Fourth International Conference on Genetic Algorithms, R. K. Belew and L. B. Booker (eds.), Morgan Kaufmann, San Mateo, CA, 1991, p.303. (c) K. DeJong and W. Spears, in Proceedings of the Fifth International Conference on Genetic Algorithms, S. Forrest (ed.), Morgan Kaufmann, San Mateo, CA, 1993, p. 618. (d) W. M. Spears, K. A. De Jong, T. Bäch, D. Fogel,

and H. de Garis, in Machine Learning, ECML-93, P. B. Bradzil (ed.), Springer, Berlin, 1993, p. 442. (e) T. Bäch and H.-P. Schwefel, Evolutionary Computation **1**, 1 (1993).

[55] A. Gonzalez-Lafont, T. N. Truong, and D. G. Truhlar, J. Chem. Phys. **95**, 8875 (1991).

[56] (a) S. P. Walch and T. H. Dunning, J. Chem. Phys. **72**, 1303 (1980). (b) G. C. Schatz and H. H. Elgersma, Chem. Phys. Lett. **73**, 21 (1980).

[57] V. S. Melissas and D. G. Truhlar, J. Chem. Phys. **99**, 3542 (1993).

[58] T. H. Dunning, Jr., J. Chem. Phys. **90**, 1007 (1989).

[59] J. A. Pople and M. A. Head-Gordon, J. Chem. Phys. **82**, 284 (1985).

[60] (a) H. S. Johnston, Gas Phase Reaction Rate Theory, Ronald Press, New York, 1966. (b) B. C. Garrett, D. G. Truhlar, and R. S. Grev, in Potential Energy Surfaces and Dynamics Calculations, D. G. Truhlar (ed.), Plenum, New York, 1981, p. 587.

[61] G. S. Hammond, J. Amer. Chem. Soc. **77**, 334 (1955).

[62] E. B. Wilson, Jr., J. C. Decius, and P. C. Cross, Molecular Vibrations, McGraw-Hill, New York, 1955.

[63] (a) J. B. Howard, J. Chem. Phys. **5**, 442 (1937). (b) J. B. Howard, J. Chem. Phys. **5**, 451 (1937). (c) B. Kirtman, J. Chem. Phys. **37**, 2516 (1962). (d) B. Kirtman, J. Chem. Phys. **41**, 775 (1964). (e) J. T. Hougen, Can. J. Phys. **42**, 1920 (1964). (f) P. R. Bunker, J. Chem. Phys. **47**, 718 (1967), **48**, 2832(E) (1968). (g) J. T. Hougen, P. R. Bunker, and J. W. C. Johns, J. Mol. Spectrosc. **34**, 136 (1970). (h) D. C. Moule and C. V. S. R. Rao, J. Mol. Spectrosc. **45**, 120 (1973). (i) G. Dellepiane, M. Gussoni, and J. T. Hougen, J. Mol. Spectrosc. **47**, 575 (1973). (j) D. Papoušek, J. M. R. Stone, and V. Špirko, J. Mol. Spectrosc. **48**, 17 (1973). (k) A. R. Hoy and P. R. Bunker, J. Mol. Spectrosc. **52**, 439 (1974).

[64] G. A. Natanson, Mol. Phys. **46**, 481 (1982).

[65] A. D. Isaacson, D. G. Truhlar, K. Scanlon, and J. Overend, J. Chem. Phys. **75**, 3017 (1981).

[66] D. G. Truhlar, F. B. Brown, R. Steckler, and A. Isaacson, in The Theory of Chemical Reaction Dynamics, D. C. Clary (ed.), Reidel, Dordrecht, 1986, p. 285.

[67] D. G. Truhlar, J. Chem. Soc. Faraday Trans. **90**, 1608 (1994).